Theoretical and Experimental Studies of Seismoelectric Conversions in Boreholes

Zhenya Zhu[1],[*], Shihong Chi[2], Xin Zhan[1] and M. Nafi Toksöz[1]

[1] *Earth Resources Laboratory, Massachusetts Institute of Technology, 42 Carleton St., Cambridge, MA 02142, USA.*
[2] *Petrophysics, ConocoPhillips, 600 North Dairy Ashford, Houston, TX 77252, USA.*

Abstract. We present theoretical and experimental studies on the effects of formation properties on seismoelectric conversions in fluid-filled boreholes. First, we derive the theoretical formulations for seismoelectric responses for an acoustic source in a borehole. Then, we compute the electric fields in boreholes penetrating formations with different permeability and porosity, and then we analyze the sensitivity of the converted electric fields to formation permeability and porosity. We also describe the laboratory results of the seismoelectric and seismomagnetic fields induced by an acoustic source in borehole models to confirm our theoretical and numerical developments qualitatively. We use a piezoelectric transducer to generate acoustic waves and a point electrode to receive the localized seismoelectric fields in layered boreholes and the electric component of electromagnetic waves in a fractured borehole model. Numerical results show that the magnitude ratio of the converted electric wave to the acoustic pressure increases with the porosity and permeability increases in both fast and slow formations. Furthermore, the converted electric signal is sensitive to the formation permeability for the same source frequency and formation porosity. Our experiments validate our theoretical results qualitatively. An acoustic wave at a fracture intersecting a borehole induces a radiating electromagnetic wave.

AMS subject classifications: 65Y10, 76Q05, 76S05, 78A25, 86A25

Key words: Seismoelectric conversions, borehole measurements, laboratory experiments, acoustic waves, borehole models.

1 Introduction

When a porous rock is saturated with an electrolyte, an electric double layer is formed at the interface between the solid and fluid: one side of the interface is negatively charged

---

[*]Corresponding author. *Email addresses:* zhenya@mit.edu (Z. Zhu), shihong.chi@conocophillips.com (S. Chi), xinzhan@mit.edu (X. Zhan), toksoz@mit.edu (M. N. Toksöz)

and the other is charged positively. Such a system is called an electric double layer (EDL). An acoustic wave propagating in the fluid-saturated formation moves the mobile ions in the EDL, and the moving ions generate an electric current. This current produces both electric and magnetic fields, which are called seismoelectric and seismomagnetic fields, respectively [8, 13].

Theoretical studies [3, 11] have confirmed the mechanism of the conversion. Inside a homogeneous, porous medium, the seismic wave induces localized seismoelectric and seismomagnetic fields. At an interface, the acoustic wave induces a radiating electromagnetic (EM) wave. Laboratory experiments [10, 15] measured the seismoelectric fields induced by acoustic waves in scaled models. Field experiments [2, 14] measured surface-to-surface seismoelectric signals. Seismoelectric borehole logging [5, 9] indicates a strong relationship between a seismoelectric response and a fracture. Hu et al. [4] simulated the electric waveforms based on the governing equations. Markov and Verzhbitskiy [7] simulated EM fields induced by acoustic multipole source in a borehole.

In this paper, we first conduct a theoretical and a numerical modeling studies of seismoelectric conversion in a borehole for monopole and dipole logging. Then we demonstrate the seismoelectric phenomena with a set of laboratory experiments. The particular geometry that we use is related to borehole measurements (e.g. acoustic/electric logging) in the earth. Laboratory models are scaled down by using the acoustic wavelength scaling. Borehole models are made to simulate a layered earth, and boreholes with a horizontal fracture. An acoustic transducer and an electrode are applied to record the acoustic wave and the electric field induced by an acoustic wave, respectively.

2   Theoretical and numerical studies

We first conduct theoretical and numerical studies of seismoelectric conversions in fluid-filled boreholes. We apply Pride's governing equations into the borehole model to conduct a theoretical study for multipole acoustic waves inducing seismoelectric fields. Both the acoustic pressure and the electric field strength are calculated by matching the mechanic and the electric boundary conditions at the borehole wall. We numerically calculate the acoustic and the seismoelectric fields generated by a monopole or a dipole acoustic source in a fast or slow formation borehole.

2.1   Mathematical formulation of the multipole seismoelectric field

According to Pride's equations [12] for seismoelectric wave propagation in porous media, the electric current density $\overline{J}$ can be written as

$$\overline{J} = \sigma \overline{E} + L\left(-\nabla p + \omega^2 \rho_f \overline{u}\right),\tag{2.1}$$

and the displacement of the fluid phase $\overline{w}$ can be expressed as

$$-i\omega \overline{w} = L\overline{E} + \frac{k}{\eta}\left(-\nabla p + \omega^2 \rho_f \overline{u}\right),\tag{2.2}$$

where $\overline{u}$ is the displacement of the solid frame, p is the pore pressure, $\overline{E}$ is the electric field strength, L is the coupling coefficient, ρ_f and η are the density and the viscosity of the pore fluid, respectively, k and σ are the dynamic permeability and conductivity of the porous medium, and ω is the angular frequency of the acoustic wave. The coupling coefficient L is defined by Pride [12] as:

$$L = -\frac{\phi}{\alpha_\infty} \frac{\zeta \varepsilon_f}{\mu} \left(1 - \frac{i\omega}{\omega_c} \frac{4}{M^2} \right)^{-\frac{1}{2}},$$ (2.3)

where ϕ is the formation porosity, α_∞ is the formation tortuosity, ζ is the zeta-potential of the electrochemical interface between pore fluid and grain surface, ε_f is the pore fluid permittivity, μ is the pore fluid viscosity, ω_c is the Biot critical frequency for the formation and M is a pore-geometry dependent dimensionless parameter (close to one for most media [6]).

Hu and Liu [4] introduced two assumptions to approximate the seismoelectric wave fields. They first showed that the converted electric field affects the elastic wave field negligibly and the coupling term in Eq. (2.2) can be ignored. They also assumed that the electric field is time invariant within the acoustic logging operation framework, because the EM wavelength is much longer than the tool length. Under this quasi-static condition, the electric field strength can be written as the gradient of an electric potential ϕ:

$$\overline{E} = -\nabla \phi.$$ (2.4)

They showed that the electric potential and the potential of the gradient field of the solid displacement are related as follows:

$$\nabla^2 \phi = \frac{L}{\sigma} \left(-\nabla^2 p + \omega^2 \rho_f \nabla^2 \varphi \right),$$ (2.5)

where φ is the displacement potential of the gradient field.

In wave number domain, the solution to Eq. (2.5) is

$$\phi_n = A_{em} K_n (k_{em} r) \cos n\theta + \frac{L}{\sigma} \left(-p + \omega^2 \rho_f \varphi \right),$$ (2.6)

where A_{em} is an unknown coefficient, k_{em} is the axial wavenumber of the EM wave. K_n ($n = 0,1,\cdots$) is the modified Bessel functions of the second kind of order n. The pore pressure can be written as:

$$p = \sum_{j=1}^{2} \left[(Q + \tilde{R}\xi_j) l_j^2 \Big/ \phi_0 \right] A_j I_n (k_{pf} r_0) K_n (k_{pj} r) \cos n\theta,$$ (2.7)

where Q, $\tilde{R}$, and ξ_j are defined by Biot [1], the wavenumber $l_j^2 = \omega^2 / \alpha_j^2$, ϕ_0 is formation porosity, A_j is a unknown coefficient, and r_0 is the radius of the circle of monopole point

source distribution. κ_{pf} and κ_{pj} are the axial wavenumbers of the acoustic waves in the fluid and in the formation. I_n and K_n ($n=0,1,\cdots$) are the modified Bessel functions of the first and second kind of order n.

The displacement potential can be written as

$$\varphi_j = A_j I_n \left(k_{pf} r_0 \right) K_n \left(k_{pj} r \right) \cos n\theta. \tag{2.8}$$

The potential function φ_j is a solution for a multipole source of order $2n$ (the multipole sources are corresponding to monopole, dipole, and quadrupole sources, when n=1, 2, and 3, respectively). The index j indicates fast or slow waves in the porous media.

We obtain the electric field using Eq. (2.4). In formation,

$$E_z = -ik_{em}\phi_n, \tag{2.9}$$

and J can be derived from Eq. (2.1).

In a borehole fluid, we assume the electric potential to be

$$\phi_f = -ik_{em} B_{em} I_n \left(k_{em} r \right) I_n \left(k_{pj} r_0 \right) \cos n\theta, \tag{2.10}$$

where coefficient B_{em} is to be determined. The electric current density in a borehole can also be derived from Eq. (2.1).

2.2 Boundary conditions at the borehole wall

Across the borehole wall, the tangential electric field and the normal magnetic field are continuous. This boundary condition is equivalent to the electric potential and the radial current continuity. We can solve for the unknown coefficients A_{em} and B_{em} by applying these boundary conditions. Finally, we can compute the electric fields in the formation and in the borehole fluid.

2.3 Numerical computation of the multipole seismoelectric field

We compute the electric field in borehole formations with high and low rock compressibility, permeability, and porosity. Fig. 1 compares the monopole and the dipole wave fields for a fast formation. Fig. 1(a) shows that P, pseudo-Rayleigh, and Stoneley wave modes, all generate local electric fields, but the Stoneley mode has the highest amplitude in the acoustic and electric fields. We study the sensitivity of the seismoelectric conversion to the formation porosity and permeability in a dipole logging (Fig. 2). Strong electric signals are induced by the flexural waves. There is a 90°-phase delay between the acoustic and the converted electric signal.

Fig. 2 shows that the seismoelectric conversion rate for the high permeability (1 darcy) in a slow formation is about 25 times higher than that for a low permeability (1 millidarcy). Here we use 30% for formation porosity.
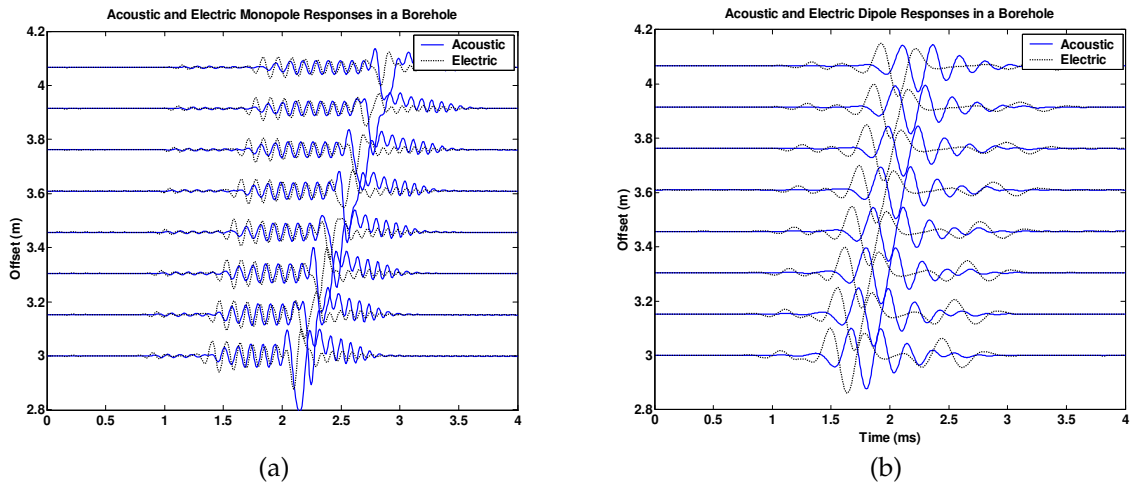
Figure 1: Comparison of monopole (a) and dipole (b) responses in a borehole. For each source, the acoustic and the electric signals are plotted on top of each other. They are 90 degree out of phase.
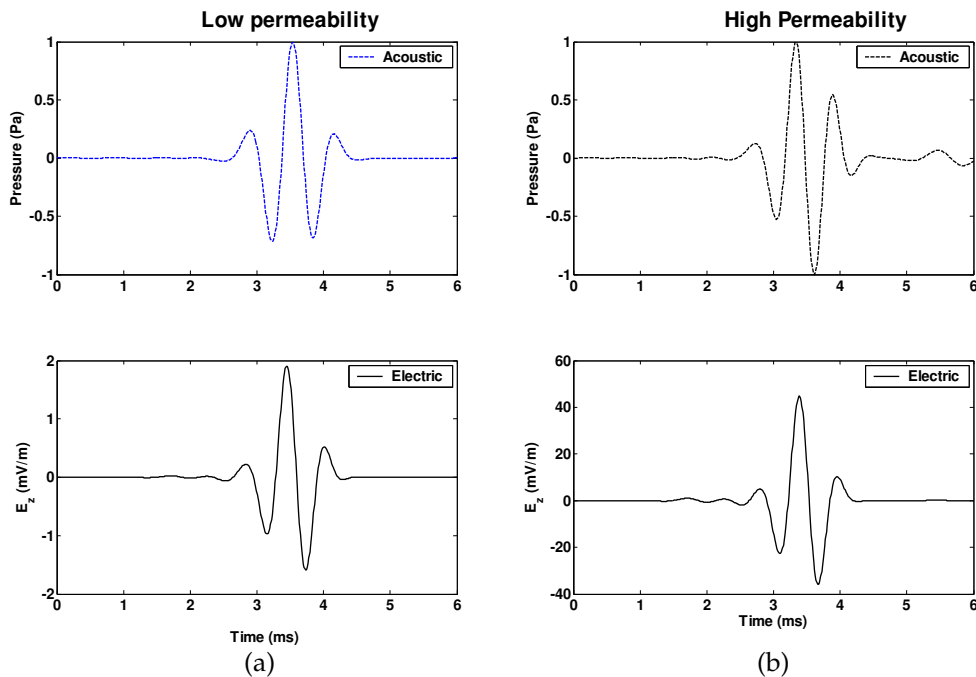

Figure 2: Comparison of the dipole responses in low (a) (1.0 millidarcy) and high (b) (1.0 darcy) permeability rocks. Note that we use different scales for the electric fields. The formation parameters are shown in Table 1. The formation porosity is 30%.

When we study the sensitivity to porosity, we fix the permeability to 100 millidarcy and vary the porosity from 5% to 30%. The slow formation (shear wave velocity is slower than compressional wave velocity of water) parameters are shown in Table 1.

Table 1: The slow formation parameters.

Ks (GPa)	Rock density (g/cm^3)	Rock Vp (km/s)	Rock Vs (km/s)
35	2.6	2.0	1.2

Fig. 3(a) shows that the conversion ratio is not very sensitive to porosity. We then fix the porosity at 20% and vary the permeability from 1 millidarcy to 1 darcy. Fig. 3(b) shows that the acoustic to the electric conversion rate increases almost linearly with the logarithm of permeability.

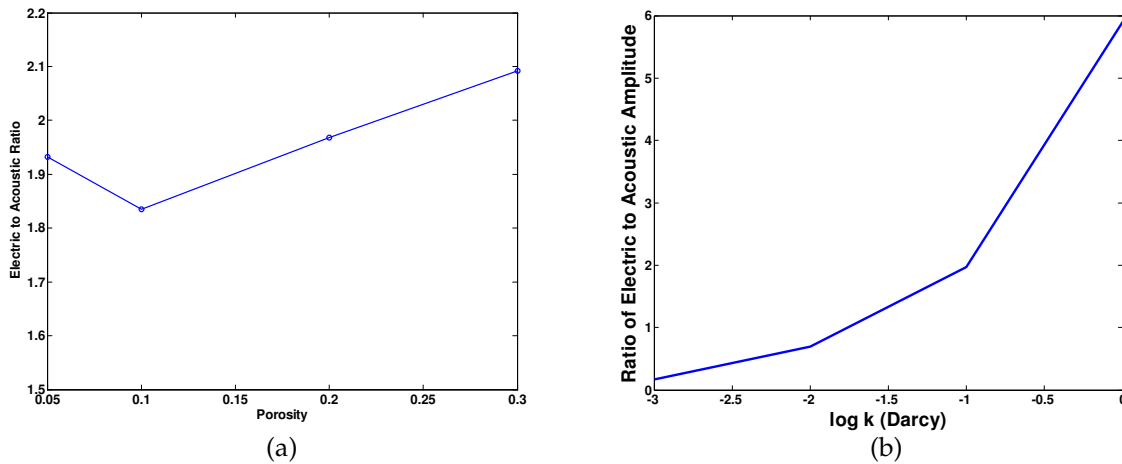(a)   (b)

Figure 3: Sensitivity of the ratio of electric to acoustic amplitude to porosity (a) and permeability (b) in the slow formation. In Fig. 3, E/P is in mv/(m.Pa) and porosity is in volume fraction.

In our numerical studies, the acoustic source frequency, ω, is centered at 1.5 kHz. The Biot critical frequencies, ω_c, for the formation parameters that we use are above 60 kHz [8]. Therefore, the frequency of the acoustic source is much lower than the Biot critical frequency. For Stoneley wave, Mikhailov et al. [8] derived a complete analytical solution for the ratio of the vertical component of the electrical field and the pressure in the borehole (E/P). Their solution indicates that at frequencies below the Biot critical frequency, E/P is proportional to porosity and is insensitive to permeability. Our studies focus on the flexural wave associated with seismoelectric phenomena. Fig. 3(a) shows a general increasing E/P with porosity, though at 10% the E/P ratio deviates from the general trend. This result agrees with the Stoneley wave theory in general. However, Fig. 3(b) shows that the electric wave accompanying the flexural wave is more sensitive to permeability than to porosity. This result does not agree with the theory for Stoneley wave. Further development for E/P conversion of higher order acoustic modes is necessary to investigate this apparent contradiction.
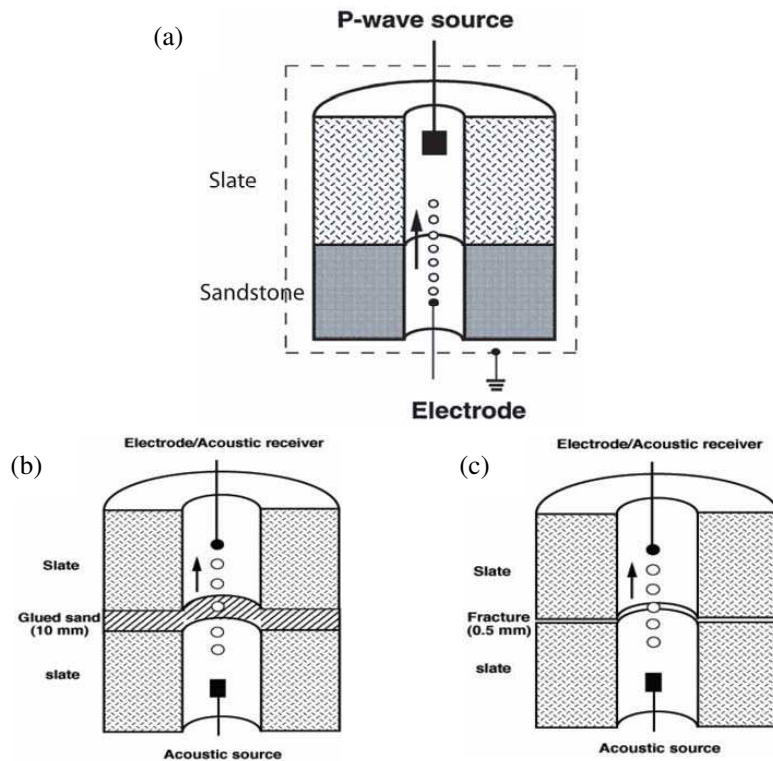
Figure 4: Schematics of borehole models and measurements. (a) The layered borehole model with slate and sandstone, (b) The sandwiched borehole model, and (c) The borehole model with a horizontal fracture of 5 mm aperture. The acoustic source is fixed in the boreholes and the receiver moves along the boreholes.

3   Laboratory experiments

Theoretical results show that the amplitudes of the electric signals induced by the seismoelectric conversion increases when the rock porosity or permeability increases. To measure the ratio of the electric to the acoustic amplitude, we make layered and sandwiched borehole models using two rocks with the different porosity and permeability. We also make a borehole model with a horizontal fracture to investigate the seismoelectric conversion at the fracture. The apparent porosity and permeability increase if there are fractures in a rock. However, the horizontal fracture changes the continuity of the borehole formation along the borehole axis.

The layered borehole model (Fig. 4(a)) was made of two materials (slate and sandstone) with a horizontal interface, but without a fracture between the layers. The porosity of sandstone and slate is about 20% and 1%, the permeability is about 50 millidarcy and less than 1 millidarcy, respectively. Fig. 4(b) shows the sandwiched borehole model with 10 mm thickness, epoxy-glued sand layer between two slate blocks. The porosity and permeability of the glued sand are about 30% and 100 darcy, respectively. There are no

fractures at the two interfaces between sand and slate blocks. Fig. 4(c) shows a fractured borehole model. A fluid-saturated horizontal fracture with a 5 mm aperture is between two slate blocks. The diameter of the boreholes is about 10 mm. The acoustic monopole source is a cylindrical, 9 mm in diameter, PZT transducer. The electric source to excite the acoustic transducer is a 750 V square pulse with a 10 μs width.

In the borehole models, we record the acoustic waves and the electric signals generated by the monopole acoustic source when the source is fixed in the slate section and an acoustic receiver or electrode moves along the boreholes (Fig. 4). When we record the acoustic waves or the electric signals, we take a 32 μs time delay to avoid the electric interference of the strong electric source, which excites the acoustic source.
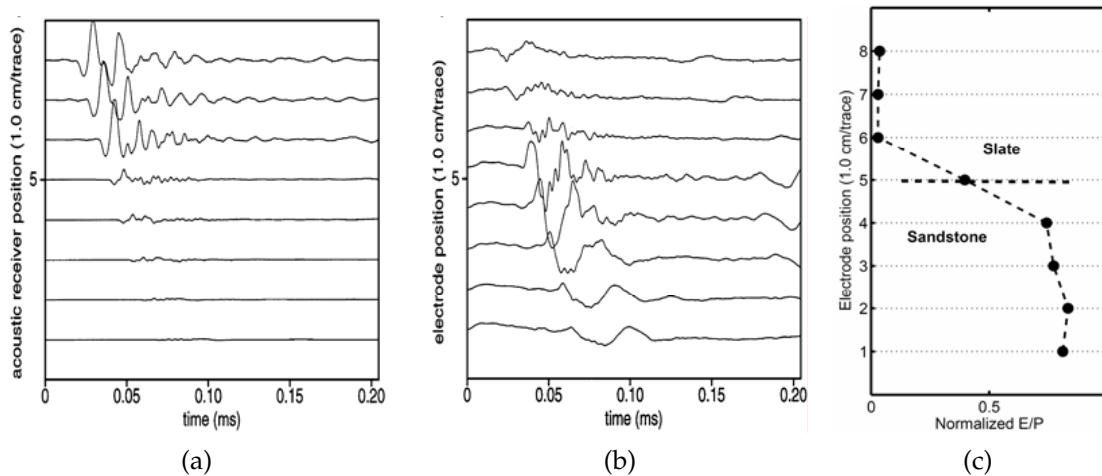

Figure 5: Acoustic waveforms (a) and electric signals (b) recorded in the layered borehole model without a horizontal fracture (Fig. 4(a)). Fig. 5(c) shows the electric amplitudes (E) normalized by the amplitudes (P) of the Stoneley wave at each trace. The interface between slate and sandstone is located at trace 5 and indicated with a horizontal dash line in (c).

Fig. 5 shows the recorded acoustic waveforms (a), the electric signals (b), and the electric amplitude normalized by the acoustic amplitude (c). The moveout of the acoustic waves and the electric signals are the same, confirming that the acoustic wave induces the localized electric field. The amplitude of the electric signals is directly proportional to the acoustic amplitude at the same condition. The electric-to-acoustic ratio (E/P) depends on the porosity and permeability in a given rock. This is demonstrated in Fig. 5(c). In the slate section, which has a low porosity and permeability, the E/P ratio is very low. On the other hand, in the sandstone section, that has higher porosity and permeability, the E/P is much higher comparing to the slate section. The ratio (E/P) in the sandstone is about 30 times higher than in the slate.

In the sandwiched borehole model, we record the Stoneley waves (Fig. 6(a)) and the seismoelectric signals (Fig. 6(b)) induced by the Stoneley waves in slate and the epoxy-glued sand. Fig. 6(c) shows the electric amplitude (E) normalized by the acoustic amplitude (P) of the Stoneley wave at each trace in the borehole. The ratio (E/P) at the glued
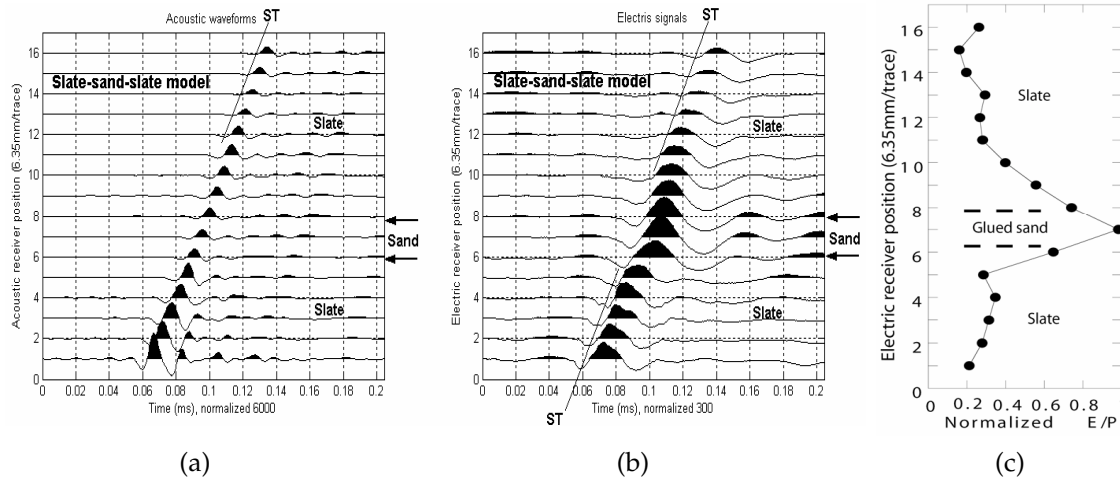
Figure 6: Acoustic waveforms (a) and electric signals (b) recorded with acoustic transducer and electrode in the sandwiched borehole model (Fig. 4(b)). The amplitude in (b) is normalized by 12 μV. Fig. 6(c) shows the electric amplitudes (E) normalized by the acoustic amplitudes (P) of the Stoneley wave at each trace. The arrows indicate the position of the glued sand sandwiched between the slate blocks. The slope of the lines ST indicates the Stoneley wave velocity in slate.

sand is about 5 times higher than that in slate.

The experimental results confirm the theoretic prediction: the seismoelectric conversion ratio is sensitive to rock permeability and porosity. Because of the limitation of the experiments, we cannot distinguish the effects of porosity and permeability on the conversion. The porous rocks with high porosity usually have high permeability. More complete sets of experiments with rocks of various porosity and permeability are necessary to distinguish the effectiveness of porosity and permeability on seismoelectric conversion. We also need further study using dipole acoustic sources to conduct our experiments to make a direct comparison with the theoretical results.

The micro-fractures in rocks not only change the local porosity and permeability, but also change the acoustic continuity in a borehole. The effects of the fractures on the seismoelectric conversion are different from the porous rocks, because the fractures do not increase the area of the fluid-solid interfaces or the electric double layer. However, a seismic wave generates a radiating EM wave at the fracture due to seismoelectric conversion [16].

When the acoustic source is fixed in the lower slate section of the fractured borehole model (Fig. 4(c)), the acoustic or the electric receiver moves gradually in the borehole and records the acoustic waveforms and the electric signals shown in Figs. 7(a) and (b). The Stoneley wave in the two slate sections induces the electric signals (Fig. 7(b)), whose apparent velocity is the same as the Stoneley wave (Fig. 7(a)).

At the horizontal fracture, the Stoneley wave induces an electromagnetic (EM) wave, whose velocity is that of an EM wave in the borehole, shown with the line of EM (traces 7-16 in Fig. 7(b)). Because the velocity of an EM wave is much faster than the acoustic
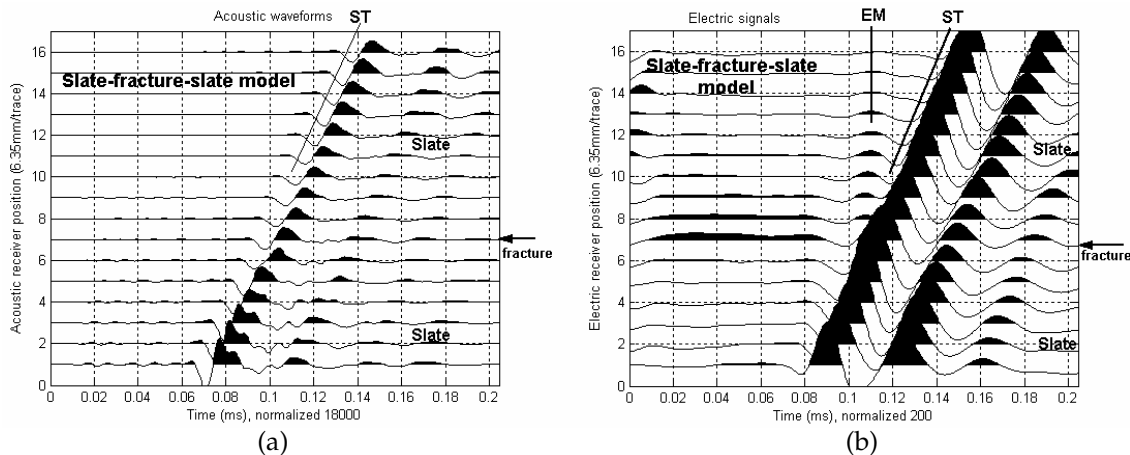
Figure 7: Acoustic waveforms (a) and electric signals (b) recorded with an acoustic transducer and an electrode in the borehole model with a horizontal fracture (Fig. 4(c)). The slope of the lines ST indicates Stoneley velocities in slate. The line EM indicates the EM wave induced at the fracture (trace 7). The arrows indicate the fracture position.

velocity, the arrival time of the EM wave is at the identical time (0.11 ms in Fig. 7(b)). The EM wave is a radiating wave and can be received at the different positions. We can see the electric component of the EM wave in traces 7-16 before the stationary electric signals (Fig. 7(b)). Any alternating electric signal always induces a magnetic signal. A Hall-effect sensor [16] can measure the magnetic signal accompanied with the stationary seismoelectric signal, but cannot measure the magnetic component of an EM wave. We may confirm that the EM wave is induced at a fracture by the propagating velocity of the electric components.

The results confirm that the acoustic waves induce stationary or localized electric and magnetic fields in a porous formation, and induce a radiating EM wave at a horizontal fracture due to its discontinuity.

Because a horizontal fracture forms a discontinuous interface on the propagation direction of the acoustic wave and the flow of the mobile charges in the fluid, the acoustic wave induces a propagating EM wave. In the homogenous sections of a borehole, acoustic waves induce a stationary or localized seismoelectric field, whose amplitudes depend on the porosity and permeability of the borehole formation.

4   Conclusions

Elastic wave propagation in fluid-saturated porous media generates electric and magnetic fields due to seismoelectric effects. The magnitudes of the converted fields depend on the formation and the fluid properties, such as permeability, porosity, conductivity, etc. We explored the possibility of using a seismoelectric measurement in a formation evaluation; we conducted theoretical modeling and laboratory measurements of seismo-

electric conversions in fluid-filled boreholes. Numerical modeling shows that the ratio of seismoelectric signal to acoustic pressure increases with increasing porosity and permeability. The converted electric signal is sensitive to formation permeability for the same acoustic source and formation porosity.

Our laboratory experiments with layered, sandwiched, and fractured borehole models show that the higher the permeability and porosity in a rock, the higher the seismoelectric ratio of electric to acoustic amplitude. These results are in agreement with the theoretical study. In a homogeneous borehole, the acoustic wave induces a localized seismoelectric field. A radiating EM wave can be generated at a discontinuity such as a fracture intersecting a borehole. Agreement between our experimental and theoretical results is very good.

Acknowledgments

References

[1] M. A. Biot, Theory of propagation of elastic waves in a fluid saturated porous rock I. low frequency range, J. Acoust. Soc. Am., 28 (1956), 179-191.
[2] K. E. Butler, R. Russell, A. Kepic and M. Maxwell, Measurement of the seismoelectric response from a shallow boundary, Geophysics, 61 (1996), 1769-1778.
[3] M. W. Haartsen, Coupled electromagnetic and acoustic wavefield modeling in poro-elastic media and its application in geophysical exploration, Ph.D. Thesis, Massachusetts Institute of Technology, 1995.
[4] H. Hu and J. Liu, Simulation of converted electric field during acoustoeletric logging, SEG Intl. Exposition and 72nd Annual Meeting, 2002.
[5] C. W. Hunt and M. H. Worthington, Borehole seismoelectric responses in fracture dominated hydraulically conductive zones, Geophys. Res. Lett., 27(9) (2000), 1315-1318.
[6] D. L. Johnson, J. Koplik and R. Dashen, Theory of dynamic permeability and tortuosity in fluid-saturated porous media, J. Fluid Mech., 176 (1987), 379-402.
[7] M. G. Markov, Simulation of the electroseismic effect produced by an acoustic multipole source in a fluid-filled borehole, SPWLA 45th Annual Logging Symposium, 2004.
[8] O. V. Mikhailov, Borehole electroseismic phenomena: Field measurements and theory, Ph.D. Thesis, Massachusetts Institute of Technology, 1998.
[9] O. V. Mikhailov, J. Queen and M. N. Toksöz, Using borehole electroseismic measurements to detect and characterize fractured (permeable) zone, Geophysics, 65 (2000), 1098-1112.
[10] F. D. Morgan, E. R. Williams and T. R. Madden, Streaming potential properties of westerly granite with applications, J. Geophys. Res., 94 (1989), 12449-12461.
[11] S. R. Pride and M. W. Haartsen, Electroseismic wave properties, J. Acoust. Soc. Am., 100 (1996), 1301-1315.

[12] S. R. Pride, Governing equations for the coupled electromagnetics and acoustics of porous media, Phys. Rev. B, 50 (1994), 15678-15696.

[13] S. R. Pride and F. Morgan, Seismoelectric dissipation induced by seismic waves, Geophysics, 56 (1991), 914-925.

[14] A. H. Thompson and G. A. Gist, Geophysical applications of seismoelectric conversion, The Leading Edge, 12 (1993), 1169-1173.

[15] Z. Zhu, M. W. Haartsen and M. N. Toksöz, Experimental studies of seismoelectric conversions in fluid-saturated porous media, J. Geophys. Res., 105 (2000), 28055-28064.

[16] Z. Zhu and M. N. Toksöz, Seismoelectric and seimomagnetic measurements in fractured borehole models, Geophysics, 70 (2005), F45-51.